

Angle resolved Cu and O photoemission intensities in CuO_2 planes

J.M. Eroles, C.D. Batista and A. A. Aligia
Centro Atómico Bariloche and Instituto Balseiro,
Comisión Nacional de Energía Atómica,
8400 Bariloche, Argentina

Using a mapping from the three-band extended Hubbard model for cuprate superconductors into a generalized $t - J$ model, and exact diagonalization of the latter in a 4×4 cluster, we determine the quasiparticle weight for destruction of a Cu or an O electrons with definite wave vector k . We also derive an approximate but accurate analytical expression which relates the O intensity with the quasiparticle weight in the generalized $t - J$ model. The k -dependence of Cu and O intensities is markedly different. In particular the O intensity vanishes for $k = (0, 0)$. Our results are relevant for the interpretation of angle-resolved photoemission experiments.

I. INTRODUCTION

While the wave vector dependence of the quasiparticle weight in quantum antiferromagnets has been studied intensively since the discovery of high- T_c superconductivity, the interest on the subject has been revived by the angle-resolved photoemission (ARPES) experiments on insulating $\text{Sr}_2\text{CuO}_2\text{Cl}_2$ ¹. Several theoretical works appeared fitting the observed dispersion using generalized $t - J$ ²⁻⁸, spin-fermion⁹ or one-band Hubbard models^{10,11}. More recently the photoemission intensities have been discussed^{5-8,10,15} and compared with previous results in the $t - J$ model¹²⁻¹⁴. In particular Lema and one of us^{6,8} and Sushkov *et al.*¹⁵, have developed two different methods to calculate the quasiparticle weight in the generalized $t - J$ or one-band Hubbard models in the strong coupling limit, using the self-consistent Born approximation (SCBA). The results of both methods, an analytical approach based on the "string picture"¹³, and exact diagonalization of a 32-site cluster⁷ were compared recently⁸. The method of Sushkov *et al.* introduces spurious low-energy peaks in the Green function which can, however, be identified and eliminated. The other SCBA method compares better with exact diagonalization and the results of the string picture underestimate the weights. However, since the operators $c_{k\sigma}^\dagger$ entering generalized $t - J$ or one-band Hubbard models are effective operators which cannot be trivially translated into Cu and O holes of the original system, the above mentioned efforts are insufficient for a comparison with experiment.

Experimental evidence about the symmetry of holes in cuprate superconductors¹⁶⁻¹⁸, as well as constrained-density functional calculations^{19,20}, justify the three-band Hubbard model H_{3b} ^{21,22} as the starting point for the description of these systems. H_{3b} contains Cu $3d_{x^2-y^2}$ and O $2p_\sigma$ orbitals. To explain some Raman^{23,24} and photoemission²⁵ experiments at excitation energies above 1eV, it is necessary to include other orbitals in the model²⁶, but these are not important for the energy scale of the ARPES experiments of Ref. 1. However, even restricting the basis to the above mentioned orbitals, the

size of the systems which can be diagonalized numerically at present, do not contain more than four unit cells²⁷. This is too small to discuss the above mentioned ARPES experiments¹. Thus, to study this problem by numerical methods at zero temperature, it is necessary to integrate out the high-energy degrees of freedom. Furthermore, analytical approximations like slave bosons give better results when applied to an appropriate low-energy Hamiltonian²⁸, and the successful SCBA cannot be applied to H_{3b} .

Several low-energy reduction procedures have been proposed²⁸⁻³⁴. Eliminating the Cu-O hopping t_{pd} by means of a canonical transformation, leads to the spin-fermion H_{sf} (or Kondo-Heisenberg) model^{29,30}. Although t_{pd} is in principle not small enough to guarantee the accuracy of the resulting H_{sf} , this effective Hamiltonian, with parameters renormalized to fit the energy levels of a CuO_4 cluster, reproduces very well optical and magnetic properties of H_{3b} in a Cu_4O_8 cluster³⁰. Also one-band generalized Hubbard^{28,29,32} and $t - J$ models^{33,34} were derived. The latter represent the highest low-energy reduction reached so far, and after the first proposal of Zhang and Rice³⁵, further work confirmed that a generalized $t - J$ model H_{GtJ} reproduces accurately the low-energy physics of the other models^{20,36-42}. In particular, projecting the Hilbert space of H_{sf} onto local (non-orthogonal) Zhang-Rice states⁴¹, mapping the model in this reduced Hilbert space to H_{GtJ} , and solving numerically the latter, we obtained a band structure and magnetic properties which agree very well with the corresponding properties calculated directly on H_{sf} ⁴². It is important to emphasize that to calculate any property of the cuprates, expressed in terms of the expectation value of an operator of H_{3b} , using an effective low-energy Hamiltonian, the mapping procedure should be extended to the operator of the quantity to be calculated^{30,32,43}, or alternatively the relevant states of the effective Hamiltonian should be mapped back onto the corresponding states of H_{3b} .

In this work we calculate the low-energy part of the Cu and O ARPES, using the low-energy reduction from H_{3b} to H_{sf} and from it to H_{GtJ} , mapping the local Zhang-

Rice singlets to vacant sites^{41,42}. The relevant operators of H_{3b} are mapped to H_{sf} , and the ground state of H_{sf} is constructed from that of H_{GtJ} in a system containing 4×4 unit cells. For the O ARPES we give a simple recipe to relate it with the quasiparticle weight in H_{GtJ} , which can be calculated with the SCBA or other analytical approaches⁸. We find significant differences between Cu and O ARPES. Since the photoemission cross-section for Cu d and O p orbitals have different dependences on the incident energy of the photon⁴⁴, these differences should be accessible to experiments.

In section II we briefly review the mapping procedure and derive the equations necessary to express the ARPES results in terms of numerical or (in some cases) analytical results on H_{GtJ} . Section III contains the results and section IV the conclusions.

II. MAPPING PROCEDURE AND RELEVANT EQUATIONS

A. Deriving the spin-fermion model from H_{3b}

Our starting point for the description of the superconducting cuprates below 1eV is the extended three-band Hubbard model. To simplify the writing we change by -1 the phases of half of the O and Cu orbitals in such a way that the hopping matrix elements do not depend on direction. The original phases should be restored in the comparison with the experimental ARPES results⁴⁵. The Hamiltonian takes the form:

$$\begin{aligned}
H_{3b} = & \epsilon_d \sum_{i\sigma} d_{i\sigma}^\dagger d_{i\sigma} + (\epsilon_d + \Delta) \sum_{j\sigma} p_{j\sigma}^\dagger p_{j\sigma} + \\
& + U_d \sum_i d_{i\uparrow}^\dagger d_{i\uparrow} d_{i\downarrow}^\dagger d_{i\downarrow} + U_p \sum_j p_{j\uparrow}^\dagger p_{j\uparrow} p_{j\downarrow}^\dagger p_{j\downarrow} + \\
& + U_{pd} \sum_{i\delta\sigma\sigma'} d_{i\sigma}^\dagger d_{i\sigma} p_{i+\delta\sigma'}^\dagger p_{i+\delta\sigma'} \\
& + t_{pd} \sum_{i\delta\sigma} [p_{i+\delta\sigma}^\dagger d_{i\sigma} + h.c.] \\
& - t_{pp} \sum_{j\gamma\sigma} p_{j+\gamma\sigma}^\dagger p_{j\sigma}
\end{aligned} \tag{1}$$

where $d_{i\sigma}^\dagger$ ($p_{j\sigma}^\dagger$) creates a hole on the Cu 3d (O 2p) orbital at site i (j). The four nearest-neighbor (next nearest-neighbor) O sites to Cu site i are denoted by $i+\delta$ ($i+\gamma$). A canonical transformation which eliminates terms linear in t_{pd} , retaining also the fourth order terms, leads to the spin-fermion model^{29,30}:

$$\begin{aligned}
H_{sf} = & \sum_{i\delta \neq \delta'\sigma} \tilde{p}_{i+\delta'\sigma}^\dagger \tilde{p}_{i+\delta\sigma} [(t_1 + t_2)(\frac{1}{2} + 2\mathbf{S}_i \cdot \mathbf{S}_{i+\delta}) - t_2] \\
& - t'_{pp} \sum_{j\gamma\sigma} \tilde{p}_{j+\gamma\sigma}^\dagger \tilde{p}_{j\sigma} + J_K \sum_{i\delta} (\mathbf{S}_i \cdot \mathbf{S}_{i+\delta} - \frac{1}{4})
\end{aligned}$$

$$+ \frac{J}{2} \sum_{i\delta} (\mathbf{S}_i \cdot \mathbf{S}_{i+2\delta} - \frac{1}{4}), \tag{2}$$

where $\tilde{p}_{j\sigma}^\dagger$ are effective O creation operators, and \mathbf{S}_i ($\mathbf{S}_{i+\delta}$) is the effective spin at Cu site i (O site $i+\delta$). Due to the fact that t_{pd} is not very small compared to Δ or $U_d - \Delta$, the expressions for the parameters of H_{sf} obtained from the canonical transformation up to fourth order in t_{pd} are not accurate enough. However, this shortcoming is avoided if the parameters of H_{sf} are renormalized to fit the energy levels of H_{3b} which in the limit $t_{pd} \rightarrow 0$ corresponds to a level of H_{sf} , in a CuO_4 cluster with one and two holes. Since the case $t_{pp} \neq 0$ has not been described before and the information is necessary for the expressions of the ARPES results, we briefly review this method.

For two holes in the CuO_4 cluster the 16 eigenstates of H_{sf} can be classified in four spin singlets and four spin triplets distributed in six energy levels: one Γ_1 (invariant under the point group operations), one Γ_3 (transforming like $x^2 - y^2$) and a doublet Γ_5 (transforming like x, y) for each total spin. The spin multiplicity $2S+1$ will be denoted in the superscript. The ground state is the invariant singlet $|g_{sf}(\Gamma_1^1)\rangle = \frac{1}{\sqrt{8}} \sum_{i\delta} (\tilde{p}_{i+\delta\uparrow}^\dagger \tilde{d}_{i\downarrow}^\dagger - \tilde{p}_{i+\delta\downarrow}^\dagger \tilde{d}_{i\uparrow}^\dagger) |0\rangle$, which represents a Zhang-Rice singlet. Each eigenstate of H_{sf} has a corresponding eigenstate of H_{3b} , which is the lowest eigenstate of a small matrix in the corresponding symmetry sector Γ_m^n . The largest matrix corresponds to Γ_1^1 and is reproduced here for future use:

$$\begin{pmatrix}
-2t_{pp} & 2t_{pd} & \sqrt{2}t_{pd} & \sqrt{2}t_{pd} & \sqrt{8}t_{pd} \\
2t_{pd} & \Delta & -2\sqrt{2}t_{pp} & -2\sqrt{2}t_{pp} & 0 \\
\sqrt{2}t_{pd} & -2\sqrt{2}t_{pp} & \Delta & 0 & 0 \\
\sqrt{2}t_{pd} & -2\sqrt{2}t_{pp} & 0 & \Delta + U_p & 0 \\
\sqrt{8}t_{pd} & 0 & 0 & 0 & U_d - \Delta - 2U_{pd}
\end{pmatrix} \tag{3}$$

The basis states of Eq.(3) are the following:

$$\begin{aligned}
|1\rangle &= \frac{1}{\sqrt{8}} \sum_{i\delta} (\tilde{p}_{i+\delta\uparrow}^\dagger \tilde{d}_{i\downarrow}^\dagger - \tilde{p}_{i+\delta\downarrow}^\dagger \tilde{d}_{i\uparrow}^\dagger) |0\rangle, \\
|2\rangle &= \frac{1}{\sqrt{8}} \sum_{i\delta} (\tilde{p}_{i+\delta\uparrow}^\dagger \tilde{p}_{i+R\delta\downarrow}^\dagger - \tilde{p}_{i+\delta\downarrow}^\dagger \tilde{p}_{i+R\delta\uparrow}^\dagger) |0\rangle, \\
|3\rangle &= \frac{1}{2} \sum_{i\delta} \tilde{p}_{i+\delta\uparrow}^\dagger \tilde{p}_{i-\delta\downarrow}^\dagger |0\rangle, \\
|4\rangle &= \frac{1}{2} \sum_{i\delta} \tilde{p}_{i+\delta\uparrow}^\dagger \tilde{p}_{i+\delta\downarrow}^\dagger |0\rangle, \\
|5\rangle &= \tilde{d}_{i\uparrow}^\dagger \tilde{d}_{i\downarrow}^\dagger |0\rangle,
\end{aligned} \tag{4}$$

where $R\delta$ is the result of rotating δ by $\pi/2$. To obtain the optimum parameters of H_{sf} , we adjust them to fit exactly the three lowest energy levels (Γ_1^1 , Γ_5^1 and Γ_5^3), the highest one (Γ_1^3), and the average of the other two ($(\Gamma_3^1 + \Gamma_3^3)/2$). Calling E_{3b} the lowest energy of H_{3b} in each symmetry sector, the result is:

$$\begin{aligned}
t'_{pp} &= \frac{E_{3b}(\Gamma_3^1) + E_{3b}(\Gamma_3^3) - E_{3b}(\Gamma_5^1) - E_{3b}(\Gamma_5^3)}{4} \\
t_1 &= \frac{E_{3b}(\Gamma_1^3) - E_{3b}(\Gamma_5^3) + 2t'_{pp}}{4} \\
t_2 &= \frac{E_{3b}(\Gamma_5^1) - E_{3b}(\Gamma_1^1)}{8} - \frac{t_1}{2} - \frac{t'_{pp}}{4} \\
J_K &= 2(t_1 + t_2) + E_{3b}(\Gamma_5^3) - E_{3b}(\Gamma_5^1)
\end{aligned} \tag{5}$$

As an example for the parameters of H_{3b} for La_2CuO_4 , obtained from constrained-density-functional approximation in Ref.²⁰ ($U_d = 10.5$, $U_p = 4.0$, $U_{pd} = 1.2$, $\Delta = 3.6$, $t_{pd} = 1.3$ and $t_{pp} = 0.6$, all energies in eV), we obtain $t'_{pp} = 0.56$, $t_1 = 0.37$, $t_2 = 0.08$, $J_K = 0.62$. The value of J , which is affected by other orbitals not included in H_{3b} ⁴⁶ is taken as $J = 0.13$ from experiment⁴⁷.

B. Mapping of the operators

We have to express the hole creation operators $d_{i\sigma}^\dagger$ and $p_{i\sigma}^\dagger$ in the basis of H_{sf} in order to calculate photoemission properties. In the lowest non-trivial order in the canonical transformation which eliminates t_{pd} , one obtains for the $d_{i\uparrow}^\dagger$ operator transformed into the spin-fermion basis³⁰:

$$d_{i\uparrow}^\dagger = a \sum_{\delta} \tilde{p}_{i+\delta\uparrow}^\dagger \tilde{n}_{i\uparrow} + b \sum_{\delta} \tilde{p}_{i+\delta\uparrow}^\dagger \tilde{n}_{i\downarrow} + c \sum_{\delta} \tilde{p}_{i+\delta\downarrow}^\dagger \tilde{d}_{i\uparrow}^\dagger \tilde{d}_{i\downarrow} \tag{6}$$

and similarly interchanging spin up and spin down, with $\tilde{n}_{i\sigma} = \tilde{d}_{i\sigma}^\dagger \tilde{d}_{i\sigma}$. The values of a , b , c which are obtained from the canonical transformation are not accurate enough. To improve them, we ask that all matrix elements of the second member of Eq. (6) between states of H_{sf} in a CuO_4 cluster with one and two holes, should coincide with the matrix elements of $d_{i\sigma}^\dagger$ between the corresponding states in H_{3b} . The result is:

$$\begin{aligned}
a &= v/2, \quad b = -u|A_5|/\sqrt{8} + (1 - |A_1|)v/4 \\
c &= u|A_5|/\sqrt{8} + (1 + |A_1|)v/4, \quad \text{with } u, v > 0 \\
u^2 &= \frac{1}{2} + \frac{\Delta + U_{pd} - 2t_{pp}}{2\sqrt{(\Delta + U_{pd} - 2t_{pp})^2 + 16t_{pd}^2}} \\
v^2 &= 1 - u^2
\end{aligned} \tag{7}$$

The A_i are the coefficients of the ground state of the matrix Eq.(3) in terms of the basis set Eq. (4): $|g_{3b}(\Gamma_1^1)\rangle = \sum_i A_i |i\rangle$.

In the lowest non-trivial order in the canonical transformation, the transformed operator of $p_{i\sigma}^\dagger$ is not changed. Following a similar procedure as above, we assume that it is a good approximation to use:

$$p_{i\sigma}^\dagger = a' \tilde{p}_{i\sigma}^\dagger \tag{8}$$

where $|a'| < 1$, because part of the spectral weight of $p_{i\sigma}^\dagger$ is distributed in high-energy states which are out of the Hilbert space of H_{sf} . Eqs.(8) and (6) were shown to be accurate enough in previous comparison of the Cu and O photoemission spectra of H_{3b} and H_{sf} in a Cu_4O_8 cluster³⁰. Here, to calculate a' , we solve exactly H_{3b} and H_{sf} in a Cu_2O cluster including and O atom and its two nearest-neighbor Cu atoms, with two and three holes. The first (second) member of Eq. (8) is applied to the $S=0$ ground state of H_{3b} (H_{sf}) with two holes. For H_{sf} , the result is a linear combination of two eigenstates with total spin $S=1/2$, which correspond to the low-energy part of the result for H_{3b} . Then, a' is determined fitting the coefficients of these two states. Inside the range of reasonable parameters of H_{3b} , we obtain $|a'|^2 \simeq 0.44$.

C. From H_{sf} to a generalized $t - J$ model

There is numerical evidence⁴⁰ that in the low-energy eigenstates of H_{sf} , the O holes are in the ground state of a CuO_4 cluster (a Zhang-Rice singlet³⁵). Defined in this way, Zhang-Rice singlets centered in nearest-neighbor Cu orbitals are non orthogonal⁴⁵. Using a projector P_2 over these non-orthogonal Zhang-Rice states⁴¹, $P_2 H_{sf} P_2$ can be mapped into a generalized $t - J$ model H_{GtJ} , in which each Zhang-Rice singlet at a CuO_4 cluster, is replaced by the vacuum (no holes) in the cluster. Retaining the most important terms, H_{GtJ} takes the form⁴¹:

$$\begin{aligned}
H_{GtJ} &= t'_1 \sum_{i\Delta\sigma} \tilde{d}_{i+\Delta\sigma}^\dagger \tilde{d}_{i\sigma} + t'_2 \sum_{i\gamma\sigma} \tilde{d}_{i+\Gamma\sigma}^\dagger \tilde{d}_{i\sigma} \\
&+ t'_3 \sum_{i\Delta\sigma} \tilde{d}_{i+2\Delta\sigma}^\dagger \tilde{d}_{i\sigma} \\
&+ t'' \sum_{i\Delta \neq \Delta'\sigma} \tilde{d}_{i+\Delta'\sigma}^\dagger \tilde{d}_{i+\Delta\sigma} (1 - 2\mathbf{S}_i \cdot \mathbf{S}_{i+\Delta}) \\
&+ \frac{J}{2} \sum_{i\Delta\sigma} \left(\mathbf{S}_i \cdot \mathbf{S}_{i+\Delta} - \frac{1}{4} \right)
\end{aligned} \tag{9}$$

where $\Delta = 2\delta$ ($\Gamma = 2\gamma$) are vectors connecting first (second) nearest-neighbor Cu atoms, and:

$$\begin{aligned}
t'_1 &= (104t'_{pp} + 246t_1 + 410t_2 + 51J_K) / 512 \\
t'_2 &= (13t'_{pp} - 11t_1) / 64 \\
t'_3 &= -11t_1 / 128 \\
t'' &= (8t_{pp} - 18t_1 - 6t_2 + 3J_K) / 256
\end{aligned} \tag{10}$$

As in H_{sf} there is an implicit constrain of forbidden double occupancy at any site. For the typical parameters of H_{3b} mentioned above, Eqs. (10) give: $t'_1 = 0.42$, $t'_2 = 0.05$, $t'_3 = 0.06$, $t'' = 0.003$.

The low-energy eigenstates $|\Psi_{sf}^\nu\rangle$ of H_{sf} can be obtained from those $|\Psi_{GtJ}^\nu\rangle$ of H_{GtJ} simply by *dressing* the vacant sites with Zhang-Rice singlets:

$$|\Psi_{sf}^\nu\rangle = \frac{T|\Psi_{GtJ}^\nu\rangle}{\langle\Psi_{GtJ}^\nu|T^\dagger T|\Psi_{GtJ}^\nu\rangle^{\frac{1}{2}}}$$

$$T = \prod_i \left[\frac{1}{\sqrt{8}} \sum_{\delta} \left(\tilde{p}_{i+\delta\uparrow}^\dagger \tilde{d}_{i\downarrow}^\dagger - \tilde{p}_{i+\delta\downarrow}^\dagger \tilde{d}_{i\uparrow}^\dagger \right) (1 - n_i) + n_i \right]$$

$$n_i = \tilde{d}_{i\uparrow}^\dagger \tilde{d}_{i\uparrow} + \tilde{d}_{i\downarrow}^\dagger \tilde{d}_{i\downarrow} \quad (11)$$

This equation, together with Eqs.(6) to (8) allow to calculate the Cu and O photoemission spectra of the three-band Hubbard model H_{3b} from the eigenstates of the corresponding generalized $t - J$ model H_{GtJ} . For the sake of clarity, and in absence of a more detailed knowledge about the experimental situation, we neglect effects of interference and the dependence on the polarization of the incident radiation and direction of the photoemitted electron. Then, in the insulating state, the Cu and O contributions to the intensity of the lowest ARPES peak are given by (the contributions for both spins are the same):

$$I_{Cu(\mathbf{k})} = 2 \left| \langle \Psi_{sf}^{\mathbf{k}} | d_{\mathbf{k}\sigma}^\dagger | \Psi_0 \rangle \right|^2$$

$$I_{O(\mathbf{k})} = 2 \left| \langle \Psi_{sf}^{\mathbf{k}} | p_{\mathbf{k}\sigma}^\dagger | \Psi_0 \rangle \right|^2 + 2 \left| \langle \Psi_{sf}^{\mathbf{k}} | p_{\mathbf{k}y\sigma}^\dagger | \Psi_0 \rangle \right|^2 \quad (12)$$

where $|\Psi_0\rangle$ is the ground state of H_{sf} and H_{GtJ} in the insulating system, $|\Psi_{sf}^{\mathbf{k}}\rangle$ the lowest energy eigenstate of H_{sf} for one added hole (which leads to a non-zero matrix element) and $d_{\mathbf{k}\sigma}^\dagger$, $p_{\mathbf{k}\sigma}^\dagger$, and $p_{\mathbf{k}y\sigma}^\dagger$, are the Fourier transforms of the three creation operators of a unit cell.

D. O intensity vs quasiparticle weight in H_{GtJ}

The formalism presented in the rest of this section allows us to calculate, in the next section, the Cu and O contributions to ARPES, from the eigenstates obtained from exact diagonalization of finite systems. To calculate the Cu part with analytical approximations applied to H_{GtJ} requires further algebraic elaboration which is beyond the scope of this work. However, as we show below, there is a simple analytical relation between the O contribution, generally the most important, and the quasiparticle weight of H_{GtJ} for one added hole. The latter quantity has been calculated accurately with the SCBA^{6,8,15} and compared with results of other analytical and numerical methods⁸.

The quasiparticle weight in H_{GtJ} is:

$$Z_\sigma(\mathbf{k}) = \left| \langle \Psi_{GtJ}^{\mathbf{k}} | \tilde{d}_{\mathbf{k}\sigma} | \Psi_0 \rangle \right|^2 \quad (13)$$

while the contribution to the intensity from, for example, $2p_x$ orbitals and spin up is (Eqs.(8),(11), and (12)):

$$I_{O\sigma}^x(\mathbf{k}) = |a'|^2 \left| \langle \Psi_0 | \tilde{p}_{\mathbf{k}\uparrow} | \Psi_{sf}^{\mathbf{k}} \rangle \right|^2$$

$$= \frac{|a'|^2 \left| \langle \Psi_0 | \frac{1}{\sqrt{N}} \sum_j e^{-ikR_j} p_{j\uparrow} T | \Psi_{GtJ}^{\mathbf{k}} \rangle \right|^2}{N_{\mathbf{k}}} \quad (14)$$

where $N_{\mathbf{k}} = |\langle \Psi_{GtJ}^{\mathbf{k}} | T^\dagger T | \Psi_{GtJ}^{\mathbf{k}} \rangle|^2$ and in \sum_j' the sum over j runs over half the O atoms (those which contains $2p_x$ orbitals or in other words, their nearest-neighbor Cu atoms lie in the x direction). The norm $N_{\mathbf{k}} \neq 1$, due to the non-orthogonality of Zhang-Rice singlets centered in nearest-neighbor Cu sites⁴¹. Since $|\Psi_{GtJ}^{\mathbf{k}}\rangle$ contains only one vacant site then $(1 - n_i)(1 - n_j)|\Psi_{GtJ}^{\mathbf{k}}\rangle = 0$ for $i \neq j$. Using this and Eq.(11) one has:

$$\tilde{p}_j T |\Psi_{GtJ}^{\mathbf{k}}\rangle = \frac{1}{2\sqrt{2}} [\tilde{d}_{j+\delta_x\downarrow}^\dagger (1 - n_{j+\delta_x}) \prod_{i \neq j+\delta_x} n_i$$

$$+ \tilde{d}_{j-\delta_x\downarrow}^\dagger (1 - n_{j-\delta_x}) \prod_{i \neq j-\delta_x} n_i] |\Psi_{GtJ}^{\mathbf{k}}\rangle$$

$$= \frac{1}{2\sqrt{2}} [\tilde{d}_{j+\delta_x\downarrow}^\dagger + \tilde{d}_{j-\delta_x\downarrow}^\dagger] |\Psi_{GtJ}^{\mathbf{k}}\rangle \quad (15)$$

where the last equality makes use of the fact that $n_i = 0$ or 1 and $\sum_i (1 - n_i) = 1$. From Eqs.(13) to (15) one obtains:

$$I_{O\uparrow}^x(\mathbf{k}) = \frac{\cos^2\left(\frac{k_x}{2}\right) |a'|^2}{2N_{\mathbf{k}}} Z_\downarrow(-\mathbf{k}) \quad (16)$$

and since from symmetry $Z_\downarrow(\mathbf{k}) = Z_\uparrow(-\mathbf{k}) = Z_\uparrow(-\mathbf{k})$, we have for the total O intensity⁴⁵:

$$I_O(\mathbf{k}) = \frac{\left(\cos^2\left(\frac{k_x}{2}\right) + \cos^2\left(\frac{k_y}{2}\right) \right) |a'|^2}{N_{\mathbf{k}}} Z_\uparrow(\mathbf{k}) \quad (17)$$

In the cluster of 4×4 unit cells, we obtain $N_{\mathbf{k}} \cong 0.36$ for all \mathbf{k} , with error less than 10%. The small dependence of the norm $T|\Psi_{GtJ}^{\mathbf{k}}\rangle$ on wave vector is to be expected in an antiferromagnetic background for realistic parameters of H_{GtJ} . As it becomes particularly clear within the string picture¹³, the motion of a vacant site in a quantum antiferromagnet can be divided into a fast motion around a fixed position on the lattice, on the scale of $\sim 3t$, against a string linear potential created by the distortion of the antiferromagnetic order, and a slow motion of the polaronic cloud, which determines the quasiparticle dispersion (with a width $\sim 2J$). $N_{\mathbf{k}}$ is clearly determined by the physics inside the polaronic cloud and is thus essentially independent of its wave vector \mathbf{k} .

From the above discussion, it is clear that the wave vector dependence of $I_O(\mathbf{k})$ is given by that of the quasiparticle weight of H_{GtJ} , and the factor $\cos^2\left(\frac{k_x}{2}\right) + \cos^2\left(\frac{k_y}{2}\right)$ ⁴⁵. This factor is very important and leads to the fact that for wave vector (π, π) in the notation of Eq. (1) ($\mathbf{k} = (0, 0)$ when the original phases are restored to compare with experiment⁴⁵), there is no O contribution to the low-energy ARPES. This is particularly clear when the on-site O repulsion $U_p = 0$. In this case, from Eq. (1), $[H_{3b}, p_{(\pi, \pi)\alpha\sigma}^\dagger] = \Delta p_{(\pi, \pi)\alpha\sigma}^\dagger$ with $\alpha = x$ or y , i.e. $p_{(\pi, \pi)\alpha\sigma}^\dagger$ does not hybridize with the Cu $3x^2 - y^2$ orbitals. Then all the O weight resides in a well defined

quasiparticle at energy $\Delta \sim 3.6$ eV, while the low-energy quasiparticles, involved in the formation of Zhang-Rice singlets, lie at negative energies (with the zero of one-particle energies of Eq.(1)²⁶).

III. RESULTS

In this section we present the result of exact diagonalization of H_{GtJ} as an effective model representing the low-energy physics of H_{3b} , in a system containing 4×4 unit cells. At the end we use Eq.(17) and previous results of $Z_\uparrow(\mathbf{k})$ to obtain $I_O(\mathbf{k})$ in larger clusters.

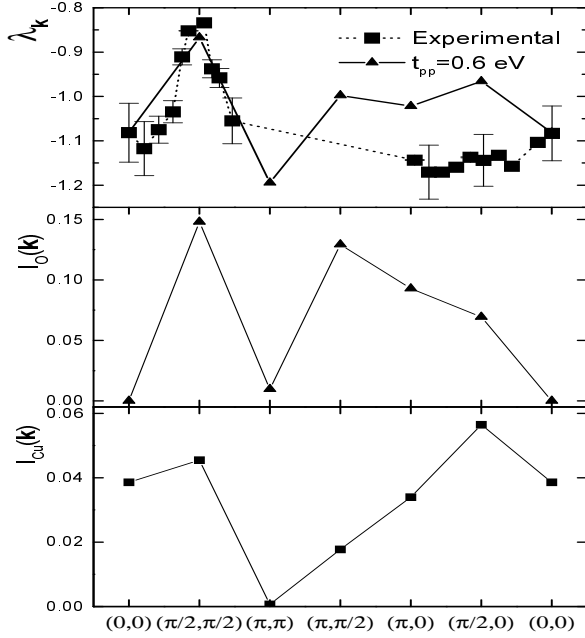


FIG. 1. Quasiparticle energies (top), oxygen intensity (middle) and Cu intensity (bottom) as a function of wave vector, for parameters of H_{3b} calculated for La_2CuO_4 ²⁰. The square symbols and error bars at the top correspond to the observed ARPES in $\text{Sr}_2\text{CuO}_2\text{Cl}_2$ ¹.

At the top of Fig. 1 we show the quasiparticle dispersion $\lambda_{\mathbf{k}}$ with the original phases restored⁴⁵ and in the electron representation (upside down with respect of the hole representation of H_{3b}), to facilitate comparison with experiment. The parameters of H_{3b} were taken from Ref.²⁰ and those of H_{GtJ} were determined from the mapping procedure, except for $J = 0.13$ which was taken from comparison with Raman experiments⁴⁷. Taking into account that there are no fitting parameters, the agreement with the experimentally measured dispersion in $\text{Sr}_2\text{CuO}_2\text{Cl}_2$ is very good. The discrepancies around $(\pi, 0)$ can be ascribed to some finite-size effects in the 4×4 cluster¹⁴, and to the fact that the parameters of H_{3b} for La_2CuO_4 ²⁰ should differ somewhat from the corresponding ones for $\text{Sr}_2\text{CuO}_2\text{Cl}_2$. A consequence of the upward shift in $\lambda_{\mathbf{k}}$ for $\mathbf{k} = (\pi, \frac{\pi}{2}), (\pi, 0)$ and $(\frac{\pi}{2}, 0)$ is

that the quasiparticle weight $Z_\sigma(\mathbf{k})$ of H_{GtJ} is exaggerated for these wave vectors⁸. This is due to the fact that for larger binding energy of the added hole, less magnons are excited and the quasiparticle is more similar to the bare hole, increasing $Z_\sigma(\mathbf{k})$.

The O and Cu intensities given by Eqs.(12) are compared in Fig. 1. As explained above, both intensities are exaggerated for wave vectors $(\pi, \frac{\pi}{2}), (\pi, 0)$ and $(\frac{\pi}{2}, 0)$. For $I_O(\mathbf{k})$ this is clear when Eq.(17)⁴⁵ with $|a'|^2/N_{\mathbf{k}} \cong 1.22$, and the weights of H_{GtJ} calculated by the SCBA^{6,8} are used. However, these finite-size effects do not affect the characteristic strong variation of the O intensity around the Σ line (joining $(0,0)$ with (π, π)). $I_O(\mathbf{k})$ is maximum for $\mathbf{k} = (\frac{\pi}{2}, \frac{\pi}{2})$ and very small for $\mathbf{k} = (\pi, \pi)$, as for the generalized $t-J$ model^{6-8,10}. However, in contrast to $Z_\sigma(\mathbf{k})$ for H_{GtJ} , $I_O(\mathbf{k})$ vanishes at $\mathbf{k} = (0,0)$. This is a consequence of the different symmetry of the p_σ and $d_{x^2-y^2}$ orbitals (or Zhang-Rice excitations) at that point, as explained (in different terms) at the end of the previous section.

In contrast to $I_O(\mathbf{k})$, the Cu intensities for $\mathbf{k} = (\frac{\pi}{2}, \frac{\pi}{2})$ and $\mathbf{k} = (0,0)$ are similar and rather large in comparison with other wave vectors. Since $I_O(0,0) = 0$, the experimental ARPES intensity at $\mathbf{k} = (0,0)$ is determined by the Cu part. The maximum of $I_{Cu}(\mathbf{k})$ for $\mathbf{k} = (\frac{\pi}{2}, 0)$ is probably not realistic for the parameters of H_{3b} which correspond to $\text{Sr}_2\text{CuO}_2\text{Cl}_2$, and should be reduced as the corresponding $\lambda_{\frac{\pi}{2},0}$ approaches the observed quasiparticle energy.

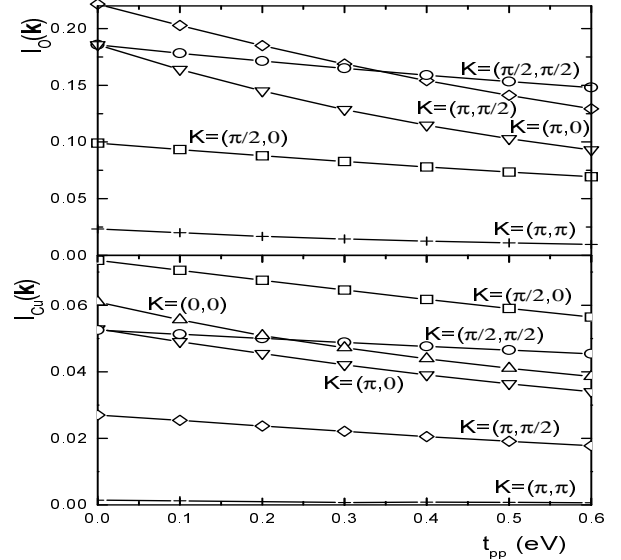


FIG. 2. Oxygen (top) and Cu (bottom) intensities for several wave vectors as a function of O-O hopping.

In Fig. 2 we show the evolution of several intensities as a function of the O-O hopping t_{pp} of H_{3b} . The importance of this term is that as t_{pp} increases, the three site term

t'' becomes positive (see Eq.(10)), particularly if t'' is obtained by fitting energy levels⁵⁰ instead of the analytical expression Eq. (10) we used here. In turn, moderate positive values of t'' favor a resonance-valence-bond superconducting ground state with (predominantly) $d_{x^2-y^2}$ symmetry^{50,51}. The effect of t_{pp} on the intensities is to reduce $I_O(\mathbf{k})$ and $I_{Cu}(\mathbf{k})$ for $\mathbf{k} = (\pi, \frac{\pi}{2})$, $(\pi, 0)$ and $(\frac{\pi}{2}, 0)$. Also $I_{Cu}(0, 0)$ decreases with t_{pp} . This is mainly a consequence of a shift downwards of the corresponding $\lambda_{\mathbf{k}}$. As a consequence, the dispersion, and also apparently the intensities, compare better with the ARPES results in $\text{Sr}_2\text{CuO}_2\text{Cl}_2$, if $t_{pp} \sim 0.6$ eV or larger.

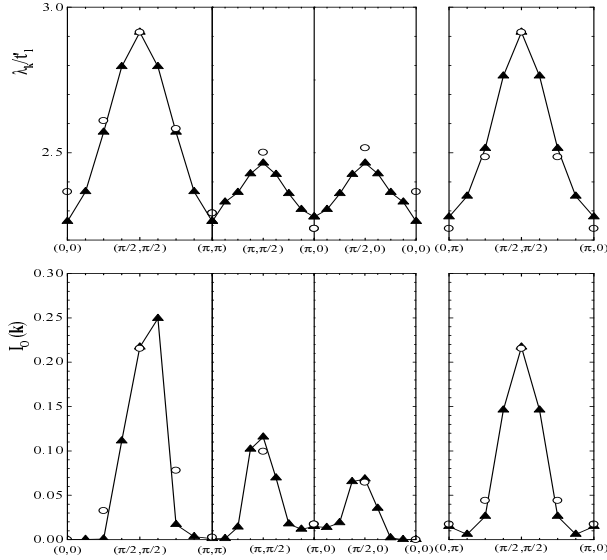


FIG. 3. Quasiparticle dispersion (top) and oxygen intensity (bottom) as a function of wave vector using exact diagonalization (open circles)⁷ and SCBA (solid triangles)⁸ results. Parameters are $J = -t'_2 = 0.3t'_1$, $t'_3 = 0.2t'_1$ and $t'' = 0$.

For the incident energy used in the ARPES experiments¹ in $\text{Sr}_2\text{CuO}_2\text{Cl}_2$, the cross section for photoemitting O $2p$ electrons is near two times that of Cu $3d$ electrons⁵². This fact and our previous results suggest that the observed intensity is given essentially by $I_O(\mathbf{k})$, except for \mathbf{k} near $(0, 0)$. We have used Eq.(17) with $N_k = 0.36$ constant, in order to relate $I_O(\mathbf{k})$ with previous accurate results for $Z_\sigma(\mathbf{k})$ in H_{GtJ} : exact diagonalization of a square cluster of 32 sites⁷, and the SCBA in a 16×16 cluster⁸. The parameters of H_{GtJ} , taken from Ref.⁷, are near the optimum ones for fitting the dispersion relation $\lambda_{\mathbf{k}}$, with $t'' = 0$. The resulting $\lambda_{\mathbf{k}}$ and $I_O(\mathbf{k})$ are shown in Fig. 3. Due to the factor $\sin^2(k_x/2) + \sin^2(k_y/2)$ ⁴⁵, the intensities along the Σ line are asymmetric and smaller near the Brillouin zone center, contrary to what was observed experimentally. We should state that a small admixture of the Cu $3d$ ¹⁰ configuration in the ground state of the undoped system (of order $t_{pd}^2/[(\Delta + U_{pd})U_d]$, which we have disre-

garded here) has the effect of increasing the Cu ARPES near $\mathbf{k} = (0, 0)$, as it is clear in the strong-coupling limit of the one-band Hubbard model (H_{1b})^{6,10,15}. However, clearly this effect is negligible on the O ARPES. The above mentioned asymmetry is even enlarged if a negative $t'' = -J/4$ (as that which comes from a canonical transformation of H_{1b}) is included^{7,8}. This suggests again that values of $t_{pp} \sim 0.6$ eV or larger, leading to positive t'' , are more realistic.

IV. CONCLUSIONS

We have developed a formalism which allows to calculate separately the low-energy part of the angle-resolved photoemission intensity from either O $2p_\sigma$ or Cu $3d_{x^2-y^2}$ orbitals, using a generalized $t - J$ model as an effective model for cuprate superconductors. This low-energy reduction is the only way to calculate the wave vector dependence of the intensities by exact diagonalization of finite systems, since at present it is not possible to diagonalize directly the three-band Hamiltonian in a periodic system large enough to contain the minimum necessary sampling of the Brillouin zone.

For the insulating system, the O intensity can be very well approximated as

$$I_O(\mathbf{k}) \cong 1.22 Z_\sigma(\mathbf{k}) (\sin^2(k_x/2) + \sin^2(k_y/2))$$

where $Z_\sigma(\mathbf{k})$ is the quasiparticle weight of the effective generalized $t - J$ model. Thus, I_O vanishes at the Γ point $\mathbf{k} = (0, 0)$. Since this is a consequence of the different symmetry of O $2p_\sigma$ states and low-energy excitations at that point, this result should persist with doping.

Our numerical results in a cluster of 4×4 unit cells, for parameters calculated for La_2CuO_4 , show that $I_O(\mathbf{k})$ is largest for $\mathbf{k} = (\frac{\pi}{2}, \frac{\pi}{2})$, and at that point, the Cu intensity $I_{Cu}(\mathbf{k})$ is nearly three times smaller. Instead while $I_{Cu}(\mathbf{k})$ has similar values at $\mathbf{k} = (\frac{\pi}{2}, \frac{\pi}{2})$ and near the Γ point, $I_O(0, 0) = 0$. The fact that $I_O(\mathbf{k})$ and $I_{Cu}(\mathbf{k})$ dominate in different regions of the Brillouin zone, makes it possible to separate both contributions experimentally. For an analysis of the experiments, as those carried out in $\text{Sr}_2\text{CuO}_2\text{Cl}_2$ ¹, the separation in Cu and O contributions is important, since the cross section for photoemitting electrons in O $2p$ or Cu $3d_{x^2-y^2}$ orbitals are different and have different dependence on the incident energy⁴⁴. For a quantitative comparison with experiment, it is necessary add the amplitudes (instead of the intensities) of the scattered waves from the three atoms per unit cell, multiplied by their respective scattering amplitudes, taking into account the polarization of the incident photons, and the direction of the photoemitted electrons. This does not require an extension of our formalism. In addition, for any particular scattering amplitudes and polarization, the expected trends can be extracted from the present results.

Agreement with the observed intensities seems to improve for $t_{pp} \geq 0.6\text{eV}$, which in turn favors an RVB ground state and d-wave superconductivity^{50,51}.

ACKNOWLEDGMENTS

Two of us (JME and CDB) are supported by the Consejo Nacional de Investigaciones Científicas y Técnicas (CONICET), Argentina. (AAA) is partially supported by CONICET.

-
- ¹ B.O. Wells, Z.-X. Shen, A. Matsuura, D.M. King, M.A. Kastner, M. Greven, and R.J. Birgeneau, Phys. Rev. Lett. **74**, 964 (1995).
 - ² A. Nazarenko, K.J.E. Vos, S. Haas, E. Dagotto, and R. Gooding, Phys. Rev. B **51**, 8676 (1995).
 - ³ V.I. Belinicher, A.L. Chernyshev, and V.A. Shubin, Phys. Rev. B **54**, 14914 (1996).
 - ⁴ T. Xiang and J.M. Wheatley, Phys. Rev. B **54**, R12653 (1996).
 - ⁵ R. Eder, Y. Ohta, and G. A. Sawatzky, Phys. Rev. B **55**, R3414 (1997).
 - ⁶ F. Lema and A.A. Aligia, Phys. Rev. B **55**, 14092 (1997).
 - ⁷ P.W. Leung, B.O. Wells and R.J. Gooding, Phys. Rev. B **56**, 6320 (1997); references therein.
 - ⁸ F. Lema and A.A. Aligia, Physica C **307**, 307 (1998).
 - ⁹ O.A. Starykh, O.F. de Alcantara Bonfim, and G. Reiter, Phys. Rev. B **52**, 12534 (1995).
 - ¹⁰ H. Eskes and R. Eder, Phys. Rev. B **54**, 14226 (1996).
 - ¹¹ F. Lema, J. Eroles, C.D. Batista and E. Gagliano, Phys. Rev. B **55**, 15289 (1997).
 - ¹² K. v. Szcepaniski, P. Horsch, W. Stephan, and M. Ziegler, Phys. Rev. B **41**, 2017 (1990); V. Elser, D.A. Huse, B.I. Shraiman, and E.D. Siggia, *ibid* **41**, 6715 (1990); E. Dagotto, R. Joynt, A. Moreo, S. Bacci, and E. Gagliano, *ibid* **41**, 9049 (1990).
 - ¹³ R. Eder and K.W. Becker, Phys. Rev. B **44**, 6982 (1991).
 - ¹⁴ D. Poilblanc, T. Ziman, H.J. Schulz, and E. Dagotto, Phys. Rev. B **47**, 14267 (1993).
 - ¹⁵ O.P. Sushkov, G.A. Sawatzky, R. Eder, and H. Eskes, Phys. Rev. B **56**, 11769 (1997).
 - ¹⁶ N. Nücker, H. Romberg, X.X. Xi, J. Fink, Gebenheimer and Z.X. Zhao, Phys. Rev. B **39**, 6619 (1989).
 - ¹⁷ M. Takigawa, P.C. Hammel, R.H. Heffner, Z. Fisk, K.C. Ott, and J.D. Thomson, Phys. Rev. Lett. **63**, 1865 (1989).
 - ¹⁸ M. Oda, C. Manabe, and M. Ido, Phys. Rev. B **53**, 2253 (1996).
 - ¹⁹ J.F. Annet, R.M. Martin, A.K. McMahan, and S. Satpathy, Phys. Rev. B **40**, 2620 (1989).
 - ²⁰ M.S. Hybertsen, E.B. Stechel, M. Schlüter, and D.R. Jennison, Phys. Rev. B **41**, 11068 (1990); references therein.
 - ²¹ C.M. Varma, S. Schmitt-Rink, and E. Abrahams, Solid State Commun. **62**, 681 (1987).
 - ²² V.J. Emery, Phys. Rev. Lett. **58**, 2794 (1987).
 - ²³ R. Liu, D. Salamon, M. Klein, S. Cooper, W. Lee, S.-W. Cheong, and D. Ginsberg, Phys. Rev. Lett. **71**, 3709 (1993).
 - ²⁴ D. Salamon, R. Liu, M. Klein, M. Karlow, S. Cooper, S.-W. Cheong, W. Lee, and D. Ginsberg, Phys. Rev. B **51**, 6617 (1995).
 - ²⁵ J.M. Pothuizen, R. Eder, M. Matoba, G. Sawatzky, N.T. Hien, and A.A. Menovsky, Phys. Rev. Lett. **78**, 717 (1997).
 - ²⁶ M.E. Simon, A.A. Aligia, C.D. Batista, E.R. Gagliano, and F. Lema, Phys. Rev. B **54**, R3780 (1996).
 - ²⁷ J. Wagner, W. Hanke, and D.J. Scalapino, Phys. Rev. B **43**, 10517 (1991).
 - ²⁸ M.E. Simon and A.A. Aligia, Phys. Rev. B **48**, 7471 (1993); references therein.
 - ²⁹ H.-B. Schüttler and A.J. Fedro, J. Appl. Phys. **63**, 4209 (1988); P. Prelovšek, Phys. Lett. A **126**, 287 (1988); J. Zaanen and A.M. Oleś, Phys. Rev. B **37**, 9423 (1988); M. Matsukawa and H. Fukuyama, J. Phys. Soc. Jpn. **58**, 2845 (1989).
 - ³⁰ C.D. Batista and A.A. Aligia, Phys. Rev. B **47**, 8929 (1993); references therein.
 - ³¹ H.-B. Schüttler and A.J. Fedro, Phys. Rev. B **45**, 7588 (1992).
 - ³² M.E. Simon, A.A. Aligia and E.R. Gagliano, Phys. Rev. B **56**, 5637 (1997); references therein.
 - ³³ L.F. Feiner, J.H. Jefferson, and R. Raimondi, Phys. Rev. B **53**, 8751 (1996); references therein.
 - ³⁴ V.I. Belinicher, A.L. Chernyshev, and L.V. Popovich, Phys. Rev. B **50**, 13768 (1994); references therein.
 - ³⁵ F.C. Zhang and T.M. Rice, Phys. Rev. B **37**, 3759 (1988).
 - ³⁶ A. Ramsak and P. Prelovšek, Phys. Rev. B **40**, 2239 (1989).
 - ³⁷ C.-X. Chen, H.-B. Schüttler and A.J. Fedro, Phys. Rev. B **41**, 2581 (1990).
 - ³⁸ T. Tohyama and S. Maekawa, J. Phys. Soc. Jpn. **59**, 1760 (1990).
 - ³⁹ S.B. Bacci, E. Gagliano, R. Martin, and J. Annet, Phys. Rev. B **44**, 7504 (1991).
 - ⁴⁰ C.D. Batista and A.A. Aligia, Phys. Rev. B **48**, 4212 (1993); **49**, 6436(E) (1994).
 - ⁴¹ A.A. Aligia, M.E. Simon, and C.D. Batista, Phys. Rev. B **49**, 13061 (1994); C.D. Batista and A.A. Aligia, Phys. Rev. B **49**, 16048 (1994).
 - ⁴² J. Eroles, C.D. Batista and A.A. Aligia, Physica C **261**, 237 (1996).
 - ⁴³ L. Feiner, Phys. Rev. B **48**, 16857 (1993).
 - ⁴⁴ J.J. Yeh and I. Lindau, Atomic Data and Nuclear Data Tables **32**, 1 (1985).
 - ⁴⁵ The change of phases by -1 in half of the O and Cu orbitals, simplifies the notations of H_{3b} , H_{sf} and several expressions of the mapping procedure. In H_{GtJ} it has the only effect of changing the sign of the nearest-neighbor hopping t'_1 . This shifts in (π, π) the one-particle wave vectors. In particular, restoring the original phases, the oxygen intensity (Eq. (17)) is proportional to $\sin^2(k_x/2) + \sin^2(k_y/2)$.
 - ⁴⁶ F. Barriquand and G.A. Sawatzky, Phys. Rev. B **50**, 16649 (1994).
 - ⁴⁷ R.R.P. Singh, P.A. Fleiry, K.B. Lyons and P.E. Sulewski, Phys. Rev. Lett. **63**, 2736 (1989); G. Blumberg *et al.*, Phys. Rev. B **53**, 11930 (1996).

- ⁴⁸ Orthogonal Zhang-Rice states can also be used in the mapping procedure^{32–35,41}, but the numerical results^{40,42,49} and an analytical comparison of both mappings⁴¹ indicates that for realistic or large O-O hopping t_{pp} , more accurate results are obtained using non-orthogonal singlets, without having to introduce higher order corrections^{33,49}.
- ⁴⁹ M.E. Simon and A.A. Aligia, Phys. Rev. B **52**, 7701 (1995).
- ⁵⁰ C.D. Batista and A.A. Aligia, Physica C **261** 237 (1996).
- ⁵¹ C.D. Batista, L.O. Manuel, H.A. Ceccatto, and A.A. Aligia, Europhys. Lett. **38**, 147 (1997); J. Low Temp. Phys. **105**, 591 (1996); F. Lema, C.D. Batista and A.A. Aligia, Physica C **259**, 287 (1996), 5637 (1997).
- ⁵² Z-X. Shen, private communication.